

A Fast Proximal Point Method for Wasserstein Distance

Yujia Xie, Xiangfeng Wang, Ruijia Wang, Hongyuan Zha

Abstract

Wasserstein distance plays increasingly important roles in machine learning, stochastic programming and image processing. Major efforts have been under way to address its high computational complexity, some leading to approximate or regularized variations such as Sinkhorn distance. However, as we will demonstrate, several important machine learning applications call for the computation of exact Wasserstein distance, and regularized variations with small regularization parameter will fail due to numerical stability issues or degrade the performance. We address this challenge by developing an Inexact Proximal point method for Optimal Transport (IPOT) with the proximal operator approximately evaluated at each iteration using projections to the probability simplex. We also simplify the architecture for learning generative models based on optimal transport solution, and generalize the idea of IPOT to a new method for computing Wasserstein barycenter. We provide convergence analysis of IPOT and experiments showing our new methods outperform the state-of-the-art methods in terms of both effectiveness and efficiency.

1 Introduction

Many practical tasks in machine learning rely on computing a Wasserstein distance between probability measures or between their sample points [ACB17, TPK⁺17]. However, the high computational cost of Wasserstein distance has been a thorny issue and has limited its application to challenging machine learning problems.

In this paper we focus on Wasserstein distance for discrete distributions the computation of which amounts to solving the following discrete *optimal transport* (OT) problem,

$$W(\boldsymbol{\mu}, \boldsymbol{\nu}) = \min_{\Gamma \in \Sigma(\boldsymbol{\mu}, \boldsymbol{\nu})} \langle \mathbf{C}, \Gamma \rangle. \quad (1)$$

Here $\boldsymbol{\mu}, \boldsymbol{\nu}$ are two probability vectors, $W(\boldsymbol{\mu}, \boldsymbol{\nu})$ is the Wasserstein distance between $\boldsymbol{\mu}$ and $\boldsymbol{\nu}$. Matrix $\mathbf{C} = [c_{ij}] \in \mathbb{R}_+^{n \times n}$ is the cost matrix, whose element c_{ij} represents the distance between the i -th support point of $\boldsymbol{\mu}$ and the j -th one of $\boldsymbol{\nu}$. Notation $\langle \cdot, \cdot \rangle$ represents the Frobenius dot-product and $\Sigma(\boldsymbol{\mu}, \boldsymbol{\nu}) = \{\Gamma \in \mathbb{R}_+^{n \times n} : \Gamma \mathbf{1}_n = \boldsymbol{\mu}, \Gamma^\top \mathbf{1}_n = \boldsymbol{\nu}\}$, where $\mathbf{1}_n$ represents n -dimensional vector of ones. This is a linear programming problem with typical super $O(n^3)$ complexity.

An effort by Cuturi to reduce the complexity leads to a regularized variation of (1) giving rise the so-called Sinkhorn distance [Cut13]. It aims to solve an entropy regularized optimal transport problem

$$W_\epsilon(\boldsymbol{\mu}, \boldsymbol{\nu}) = \min_{\Gamma \in \Sigma(\boldsymbol{\mu}, \boldsymbol{\nu})} \langle \mathbf{C}, \Gamma \rangle + \epsilon h(\Gamma). \quad (2)$$

The entropic regularizer $h(\Gamma) = \sum_{i,j} \Gamma_{ij} \ln \Gamma_{ij}$ results in an optimization problem (2) that can be solved efficiently by iterative Bregman projections [BCC⁺15],

$$\mathbf{a}^{(l+1)} = \frac{\boldsymbol{\mu}}{\mathbf{G}\mathbf{b}^{(l)}} \quad \mathbf{b}^{(l+1)} = \frac{\boldsymbol{\nu}}{\mathbf{G}^\top \mathbf{a}^{(l+1)}}$$

starting from $\mathbf{b}^{(0)} = \frac{1}{n} \mathbf{1}_n$, where $\mathbf{G} = [G_{ij}]$ and $G_{ij} = e^{-C_{ij}/\epsilon}$. The optimal solution Γ^* then takes the form $\Gamma_{ij}^* = a_i G_{ij} b_j$. The iteration is also referred as *Sinkhorn iteration*, and the method is referred as *Sinkhorn algorithm* which, recently, is proven to achieve a near- $O(n^2)$ complexity [AWR17].

The choice of ϵ has two distinct numerical implications. On one hand, $G_{ij} = e^{-C_{ij}/\epsilon}$ and if ϵ is very small, \mathbf{G} tends to underflow. The methods in [CPSV16, BCC⁺15] try to address this numerical instability by performing the computation in log-space, but they require a significant amount of extra exponential and logarithmic operations, and thus, reducing the efficiency. More

significantly, even with the benefits of log-space computation, the linear convergence rate of the Sinkhorn algorithm is determined by the *contraction ratio* $\kappa(\mathbf{G})$, which approaches 1 as $\epsilon \rightarrow 0$ [FL89]. Consequently, we observe drastically increased number of iterations for Sinkhorn method when using small ϵ .

Can we just employ Sinkhorn distance with a moderately sized ϵ for machine learning problems so that we can get the benefits of the reduced complexity? Some applications show Sinkhorn distance can generate good results with a moderately sized ϵ [GPC17, MHAH⁺16]. However, we show that in several important problems such as generative model learning and Wasserstein barycenter computation, the best performance is achieved with the original Wasserstein distance, and a moderately sized ϵ will significantly degrade the performance while the Sinkhorn algorithm with a very small ϵ becomes prohibitively expensive. More significantly, the use of IPOT in generative model learning has a critical positive ripple effect in reducing the overall complexity, further demonstrating its superiority over Sinkhorn distance.

In this paper, we propose a new framework to compute the Wasserstein distance using generalized proximal point iterations. The proximal operator is based on Bregman divergence, and its numerical evaluation can be accomplished by a Sinkhorn-like iterative process. To enhance efficiency, we can terminate the inner iteration only after a few iterations (in fact, one inner iteration is used in our numerical experiments), leading to an inexact proximal point method which is referred as Inexact Proximal point method for Optimal Transport (IPOT). Different from existing Sinkhorn algorithms, our IPOT method solves the original optimal transport problem, rather than its regularized approximation, while its computational complexity is comparable to the Sinkhorn algorithm with a moderately sized ϵ .

We first apply IPOT to generative model learning (see section 5), and contrast our method with the one based on Sinkhorn algorithm [GPC17]. The use of Wasserstein distance enabled by IPOT addresses two problems of the existing method. One problem relates to the learning performance: the smoothness introduced by entropic regularization used in Sinkhorn distance tends to shrink the learned distribution towards the mean of target distribution, and hence cannot cover the support of the target distribution adequately.¹ The other problem relates to computational complexity as well as the learning performance, the use of Sinkhorn distance entails the computation of the gradient of the optimal solution with respect to the model parameters. This requires back-propagation into the Sinkhorn iterations with increased costs, largely limiting the number of Sinkhorn iterations which affects the accuracy. Taking gradient of a computed result can further propagate numerical errors. In IPOT, we bypass back-propagation into iterations by way of leveraging the *envelop theorem*.

We then focus on the computation of Wasserstein barycenter, again we show better performance is obtained by using Wasserstein distance (with much sharper images) rather than the Sinkhorn distance. We develop a new method to compute Wasserstein barycenter by extending the idea of IPOT (see Section 6). It turns out that the inexact evaluation of the proximal operator blends well with Sinkhorn-like barycenter iteration.

Regarding IPOT, we carefully analyze its convergence behavior both in terms of theoretical analysis and empirical experiments. We also provide conditions on the number of inner iterations that will guarantee the linear convergence of IPOT. In fact, empirically, IPOT behaves better than our theoretical analysis: the algorithm seems to be convergent with just one inner iteration, demonstrating its efficiency.

2 Preliminaries

2.1 Wasserstein Distance and Optimal Transport

Wasserstein distance is a metric for two probability measures. Given two distributions μ and ν , the p -Wasserstein distance between them is defined as

$$W_p(\mu, \nu) := \left\{ \inf_{\gamma \in \Sigma(\mu, \nu)} \int_{\mathcal{M} \times \mathcal{M}} d^p(x, y) d\gamma(x, y) \right\}^{\frac{1}{p}}, \quad (3)$$

where $\Sigma(\mu, \nu)$ is the set of joint distributions whose marginals are μ and ν , respectively. The above optimization problem is also called the Monge-Kantorovitch problem or *optimal transport*

¹This is a problem related to the mode dropping or mode collapsing issues in generative model learning.

problem [Kan42]. In the following, we focus on the 2-Wasserstein distance, and for convenience we write $W = W_2^2$.

In the discrete cases, where both μ and ν represent two different probabilistic distributions on n support points, we can represent the distributions as vectors $\boldsymbol{\mu}, \boldsymbol{\nu} \in \mathbb{R}_+^n$, where $\|\boldsymbol{\mu}\|_1 = \|\boldsymbol{\nu}\|_1 = 1$. Then the Wasserstein distance is computed by (1) [GPC17, BJGR17]. In particular, given samples $\{x_i\}$ and $\{y_i\}$, we have empirical distributions $\hat{\mu} = \frac{1}{|\{x_i\}|} \sum_{x_i} \delta_{x_i}$ and $\hat{\nu} = \frac{1}{|\{y_i\}|} \sum_{y_i} \delta_{y_i}$, respectively, where $|\cdot|$ is the cardinality of a set. The supports of $\hat{\mu}$ and $\hat{\nu}$ are finite, so the samples are readily used as the support points, and we have $\boldsymbol{\mu} = \frac{1}{|\{x_i\}|} \mathbf{1}_{|\{x_i\}|}$, $\boldsymbol{\nu} = \frac{1}{|\{y_i\}|} \mathbf{1}_{|\{y_i\}|}$, and $\mathbf{C} = [c(x_i, y_j)] \in \mathbb{R}_+^{|\{x_i\}| \times |\{y_i\}|}$ in (1).

The optimization problem (1) is a linear programming (LP) problem. LP tends to provide a sparse solution, which is preferable in applications like histogram calibration or color transferring [RFP14]. However, the cost of LP scales at least $O(n^3 \log n)$ for general metric, where n is the number of support points [PW09]. As aforementioned, an alternative optimization method is the Sinkhorn algorithm in [Cut13]. Following the same strategy, many variants of the Sinkhorn algorithm have been proposed [DOT17, TCDP17, AWR17]. Unfortunately, all these methods only approximate original optimal transport by its regularized version and their performance both in terms of numerical stability and computational complexity is very sensitive to the choice of ϵ . More importantly, for certain machine learning problems employing Wasserstein distance, the use of the Sinkhorn distance tends to degrade the learning performance.

2.2 Proximal Point Method

Proximal point methods are widely used in optimization [Afr71, Roc76b, Roc76a, PB⁺14]. Since we are dealing with Problem (1), we focus on its convex programming formulation. Given a convex objective function f defined on \mathcal{X} with optimal solution set $\mathcal{X}^* \subset \mathcal{X}$, we can generate a sequence $\{x^{(t)}\}_{t=1,2,\dots}$ by the following generalized proximal point iterations:

$$x^{(t+1)} = \arg \min_{x \in \mathcal{X}} f(x) + \beta^{(t)} d(x, x^{(t)}), \quad (4)$$

where d is a regularization term used to define the proximal operator, usually defined to be a closed proper convex function. Commonly, d is defined as the square of Euclidean distance, i.e., $d(x, y) = \|x - y\|_2^2$.

The proximal point method has many advantages, e.g, it has a robust convergence behavior — a fairly mild condition on β guarantee its convergence and the specific choice of β generally just affects its convergence rate. Moreover, even if the proximal operator defined in (4) is not exactly evaluated in each iteration, for example the optimization problem (4) is only solved approximately, giving rise to inexact proximal point methods, the global convergence of which with local linear rate is still guaranteed under certain conditions [SS01, SRB11].

3 Bregman Divergence Based Proximal Point Method

3.1 Proposed Method

Our key idea is to use Bregman divergence D_h as the regularization in evaluating the proximal operator in (4), i.e.

$$\boldsymbol{\Gamma}^{(t+1)} = \arg \min_{\boldsymbol{\Gamma} \in \Sigma(\boldsymbol{\mu}, \boldsymbol{\nu})} \langle \mathbf{C}, \boldsymbol{\Gamma} \rangle + \beta^{(t)} D_h(\boldsymbol{\Gamma}, \boldsymbol{\Gamma}^{(t)}), \quad (5)$$

where Bregman divergence D_h based on entropy function $h(x) = \sum_i x_i \ln x_i$ takes the form (see supplementary material for more)

$$D_h(\mathbf{x}, \mathbf{y}) = \sum_{i=1}^n x_i \log \frac{x_i}{y_i} - \sum_{i=1}^n x_i + \sum_{i=1}^n y_i.$$

Substituting Bregman divergence into proximal point iteration (5), with simplex constraints, we obtain

$$\boldsymbol{\Gamma}^{(t+1)} \arg \min_{\boldsymbol{\Gamma} \in \Sigma(\boldsymbol{\mu}, \boldsymbol{\nu})} \langle \mathbf{C} - \beta^{(t)} \log \boldsymbol{\Gamma}^{(t)}, \boldsymbol{\Gamma} \rangle + \beta^{(t)} h(\boldsymbol{\Gamma}). \quad (6)$$

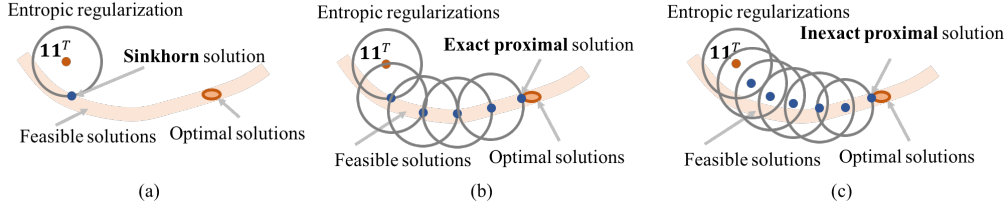


Figure 1: Schematic of the convergence path of (a) Sinkhorn algorithm, (b) exact proximal point algorithm and (c) inexact proximal point algorithm. The distance shown is in Bregman sense. Sinkhorn solution is feasible and the closest to optimal solution set within the D_h constraints. Proximal point algorithm, however, solves optimization with D_h constraints iteratively, until an optimal solution is reached.

Denote $\mathbf{C}' = \mathbf{C} - \beta^{(t)} \ln \Gamma^{(t)}$. The optimization (6) can be solved by Sinkhorn iteration by replacing G_{ij} by $G'_{ij} = e^{-C'_{ij}/\beta^{(t)}} = \Gamma^{(t)}_{ij} e^{-C_{ij}/\beta^{(t)}}$.

Figure 1 illustrates how the accuracy improves w.r.t. proximal point iterations in the solution space. First, let's consider Sinkhorn algorithm. The loss function of Sinkhorn has regularization term $\epsilon h(\Gamma)$, which can be rewritten as constraint $D_h(\Gamma, \mathbf{1}\mathbf{1}^T) \leq \eta$ for some $\eta > 0$. So in the left figure Sinkhorn solution is feasible within the D_h constraints and the closest to optimal solution set. Proximal point algorithm, on the other hand, solves optimization with D_h constraints iteratively, until an optimal solution is reached. Exact proximal point method is when (6) solved exactly. It provides a feasible solution that is closest to the optimal solution set in each step, and finally reach an optimal solution. Inexact proximal point method is when (6) is solved inexactly. Since we use Sinkhorn iteration to solve (6), this is when the iteration number of the inner optimization is not enough to converge. In each step, the solution might not be feasible or closest to the optimal set, but eventually it converges to an optimal solution.

The algorithm is shown in algorithm 1. For simplicity we use $\beta = \beta^{(t)}$. Denote $\text{diag}(\mathbf{a})$ the diagonal matrix with a_i as its i th diagonal elements. Denote \odot as element-wise matrix multiplication and \oslash as element-wise division. We use warm start to improve the efficiency, i.e. in each proximal point iteration, we use the final value of \mathbf{a} and \mathbf{b} from last proximal point iteration as initialization instead of $\mathbf{b}^{(0)} = \mathbf{1}_m$.

Later we will show empirically IPOT will converge under a large range of β with $L = 1$, a single inner iteration will suffice.

Algorithm 1 IPOT

- 1: **Input:** Probabilities $\{\boldsymbol{\mu}, \boldsymbol{\nu}\}$ on grids $\{x_i\}_{i=1}^m, \{y_j\}_{j=1}^n$
 - 2: $\mathbf{b} \leftarrow \frac{1}{m} \mathbf{1}_m$
 - 3: $C_{ij} \leftarrow c(x_i, y_j) = \|x_i - y_j\|_2^2$
 - 4: $G_{ij} \leftarrow e^{-\frac{C_{ij}}{\beta}}$
 - 5: $\Gamma^{(1)} \leftarrow \mathbf{1}\mathbf{1}^T$
 - 6: **for** $t = 1, 2, 3, \dots$ **do**
 - 7: $\mathbf{Q} \leftarrow \mathbf{G} \odot \Gamma^{(t)}$
 - 8: **for** $l = 1, 2, 3, \dots, L$ **do** // Usually set $L = 1$
 - 9: $\mathbf{a} \leftarrow \frac{\boldsymbol{\mu}}{\mathbf{Q}\mathbf{b}}, \mathbf{b} \leftarrow \frac{\boldsymbol{\nu}}{\mathbf{Q}^T\mathbf{a}}$
 - 10: **end for**
 - 11: $\Gamma^{(t+1)} \leftarrow \text{diag}(\mathbf{a})\mathbf{Q}\text{diag}(\mathbf{b})$
-

3.2 Theoretical Convergence Analysis

When the optimization problem (6) is solved exactly, we have a linear convergence rate guaranteed by the following theorem.

Theorem 3.1. *Let $\{x^{(t)}\}$ be a sequence generated by the proximal point algorithm*

$$x^{(t+1)} = \arg \min_{x \in \mathcal{X}} f(x) + \beta^{(t)} D_h(x, x^{(t)}),$$

where f is continuous and convex. Assume $f^* = \min f(x) > -\infty$. Then, with $\sum_{t=0}^{\infty} \beta^{(t)} = \infty$, we have

$$f(x^{(t)}) \downarrow f^*.$$

If we further assume f is linear and \mathcal{X} is bounded, the algorithm has linear convergence rate.

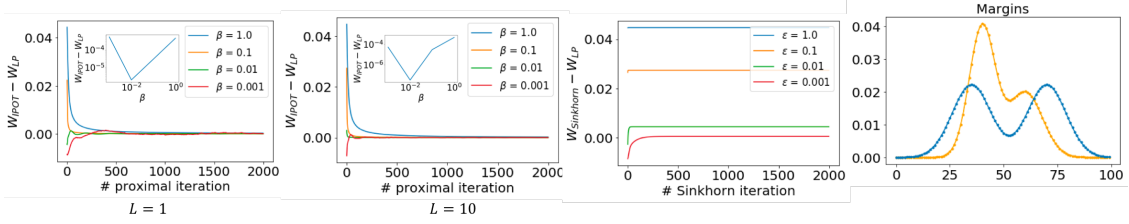


Figure 2: The left three figures show plot of differences in computed Wasserstein distances w.r.t. number of iterations. Here, W_{IPOT} and $W_{Sinkhorn}$ are the Wasserstein distance computed by IPOT and Sinkhorn method, respectively. W_{LP} is computed by simplex method, and is used as ground truth. To better demonstrate how the difference in computed WD changes w.r.t. β , we plot a mini-figure in each figure showing the information at 1000 iterations. The right figure is the two input margins for the test.

More importantly, the following theorem gives us a guarantee of convergence when (6) is solved inexactly.

Theorem 3.2. *Let $\{x^{(t)}\}$ be the sequence generated by the Bregman distance based proximal point algorithm with inexact scheme (i.e., finite number of inner iterations are employed). Define an error sequence $\{e^{(t)}\}$ where*

$$e^{(t+1)} \in \beta^{(t)} \left[\nabla f(x^{(t+1)}) + \partial \iota_{\mathcal{X}}(x^{(t+1)}) \right] + \left[\nabla h(x^{(t+1)}) - \nabla h(x^{(t)}) \right],$$

where $\iota_{\mathcal{X}}$ is the indicator function of set \mathcal{X} . If the sequence $\{e^k\}$ satisfies $\sum_{k=1}^{\infty} \|e^k\| < \infty$ and $\sum_{k=1}^{\infty} \langle e^k, x^{(t)} \rangle$ exists and is finite, then $\{x^{(t)}\}$ converges to x^{∞} with $f(x^{\infty}) = f^*$. If the sequence $\{e^{(t)}\}$ satisfies that exist $\rho \in (0, 1)$ such that $\|e^{(t)}\| \leq \rho^t$, $\langle e^{(t)}, x^{(t)} \rangle \leq \rho^t$ and with assumptions that f is linear and \mathcal{X} is bounded, then $\{x^{(t)}\}$ converges linearly.

The proof of both theorems is given in the supplementary material. Theorem 3.2 guarantees the convergence of inexact proximal point method — as long as L satisfies the given conditions, the IPOT algorithm would converge linearly. In the experimental section, we will verify our theoretical analysis and show the superiority of IPOT.

4 Empirical Analysis

In this section we will illustrate the convergence behavior of IPOT under a large range of β with $L = 1$. The scalability of IPOT is approximately the same as Sinkhorn algorithm. We leverage the implementation of Sinkhorn iteration based on Python package POT [FC17].

4.1 Convergence w.r.t. β and L

Figure 2 shows how the computed Wasserstein distances change w.r.t. the number of iterations. The input distributions used are shown in the right figure. We choose the computed Wasserstein distance $\langle \mathbf{I}, \mathbf{C} \rangle$ as the indicator of convergence, because while the optimal transportation map might not be unique, the computed Wasserstein distance at convergence must be unique and minimized to ground truth.

The left two figures describe the convergence behavior of IPOT. IPOT method is the coupling of proximal point iteration and the inner Sinkhorn iteration. On one hand, as we show in supplement material, a smaller β usually lead to quicker convergence of proximal point iterations. On the other hand, the convergence of inner Sinkhorn iteration, is quicker when β is large. Therefore, the choice of β is a trade-off between inner and outer convergence rates. The convergence rate increases w.r.t. β when β is small, and decreases when β is large. For comparison, the right figure shows the convergence path of Sinkhorn iteration. The result cannot converge to ground truth because the method is essentially regularized.

The choice of L also appears to be a trade-off. While a larger L takes more resources in each step, it also achieves a better accuracy, so less proximal point iterations are needed to converge. However, unlike β , the resources taken by increasing L is monotonously increasing in most cases according to tests. From now on, all the tests adopt $L = 1$.

4.2 Sparsity of the Transportation Map

Figure 3 describes the transportation maps of optimal transport. The maps are generated with the same input as figure 2 (shown in the right figure).

A larger ϵ leads to more blur in the Sinkhorn maps. In applications such as histogram calibration and color transferring, the non-sparse structure of transportation map make it difficult to extract the map from source distribution to target distribution. While in IPOT iteration, the result always converge to ground truth with enough iteration. On the other hand, a smaller ϵ needs significantly more iterations to converge. The Sinkhorn $\epsilon = 0.0001$ case still cannot converge after 2000 iterations.

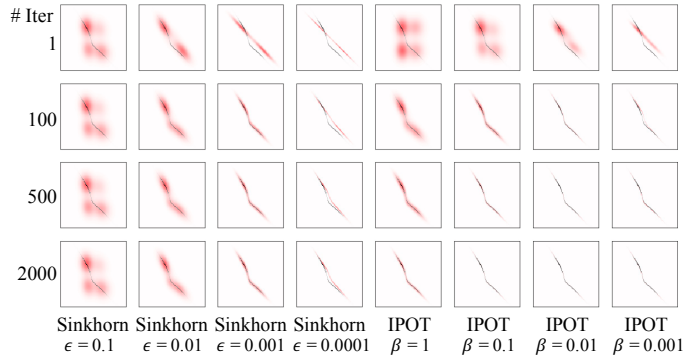


Figure 3: The transportation map generated by Sinkhorn and IPOT methods at different iteration number. The red colormap is the result from Sinkhorn or IPOT method, while the black wire is the result of simplex method for comparison. In the right lower maps, the red and the black is almost identical.

4.3 Scalability

The scalability test of IPOT is shown in figure 4. The two probability measures tested are the empirical distributions (described in Section 2.1) of uniformly distributed data. The Sinkhorn algorithm follows [Cut13] and the stabilized Sinkhorn algorithm follows [CPSV16]. We also notice there is a method [Sch16] for ϵ scaling, to help the convergence when $\epsilon \rightarrow 0$. However, although it is faster than Sinkhorn method when data size is smaller than 1024, the time used at 1024 is already around 2000s. Therefore we do not spend time on it. We do not include LP methods for comparison. Readers who are interested please refer to experiments in [Cut13], which show the efficiency improvement of Sinkhorn from algorithms based on LP is several order of magnitude.

IPOT takes approximately the same resources as Sinkhorn at $\epsilon = 0.01$, and outperforms it when $\epsilon \rightarrow 0$. From $\epsilon = 10^{-2}$ to $\epsilon = 10^{-4}$, the number of iterations needed for the same precision increases at least 10 times in Sinkhorn algorithm. If stabilized method is adopted, Sinkhorn can be even more expensive.

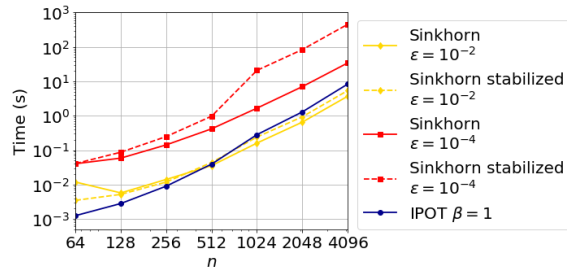


Figure 4: Log-log plot of average time used to achieve $1e-4$ relative precision. Each point is obtained by the average of 10 tests based on different datasets. The same single CPU is used for all tests.

5 Extension to Learning Generative Models

The WGAN method [ACB17] uses Wasserstein distance in learning generative models. With Wasserstein distance as the loss function, the generative networks are more stable and easier to train. The IPOT algorithm provides an alternative way to compute the Wasserstein distance than the method used by WGAN that is based on a dual formulation.

In practice, we are given a dataset $\{x_i\}$ and a source of noise data $\{z_j\}$ [GPAM⁺14]. Our goal is to find a parameterized function $g_\theta(\cdot)$ that minimize $W(\{x_i\}, \{g_\theta(z_j)\})$, where g is parameterized with parameter θ . Usually, g is parameterized by a neural network, and the minimization over θ is done by stochastic gradient descent.

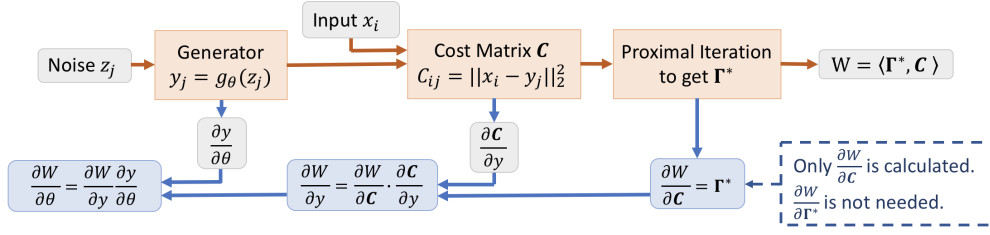


Figure 5: The architecture of the learning model using envelop theorem. According to envelop theorem, $\frac{\partial W}{\partial \Gamma^*}$ does not need to be computed, so we do not need to back-propagate into the iteration.

This problem can be solved by alternating optimization. In particular, given current estimation θ , we can obtain optimum Γ^* by our proximal point method, and compute the Wasserstein distance by $\langle \mathbf{C}(\theta), \Gamma^* \rangle$ accordingly. For simplicity, we assume $|\{x_i\}| = |\{z_j\}| = n$. As stated in section 2.1, we can modify the optimization problem as

$$W(\{x_i\}, \{g_\theta(z_j)\}) = \min_{\Gamma} \langle \mathbf{C}(\theta), \Gamma \rangle \quad \text{s.t.} \quad \Gamma \mathbf{1}_n = \frac{1}{n} \mathbf{1}_n, \Gamma^T \mathbf{1}_n = \frac{1}{n} \mathbf{1}_n, \quad (7)$$

where $\mathbf{C}(\theta) = [c(x_i, g_\theta(z_j))]$.

Then, we can further update θ by solving (7) with fixed Γ^* . Usually, the minimization over θ can be achieved by stochastic gradient descent, which involves the derivative of Wasserstein distance. Based on the below envelope theorem [Afr71], we can compute the derivative of Wasserstein distance efficiently.

Theorem 5.1. Envelope theorem. Let $f(x, \theta)$ and $l(x)$ be real-valued continuously differentiable functions, where $x \in \mathbb{R}^n$ are choice variables and $\theta \in \mathbb{R}^m$ are parameters. Denote x^* to be the optimal solution of f with constraint $l = 0$ and fixed θ , i.e.

$$x^* = \arg \min_x f(x, \theta) \quad \text{s.t.} \quad l(x) = 0.$$

Then, assume that V is continuously differentiable function defined as $V(\theta) \equiv f(x^*(\theta), \theta)$, the derivative of V over parameters is

$$\frac{\partial V(\theta)}{\partial \theta} = \frac{\partial f}{\partial \theta}.$$

In our case, because Γ^* is the minimization of $\langle \Gamma, \mathbf{C}(\theta) \rangle$ with constraints, we have

$$\begin{aligned} \frac{\partial W(\{x_i\}, \{g_\theta(z_j)\})}{\partial \theta} &= \frac{\partial \langle \Gamma^*, \mathbf{C}(\theta) \rangle}{\partial \theta} \\ &= \langle \Gamma^*, \frac{\partial \mathbf{C}(\theta)}{\partial \theta} \rangle = \langle \Gamma^*, 2(g_\theta(z_j) - x_i) \frac{\partial g_\theta(z_j)}{\partial \theta} \rangle, \end{aligned}$$

where we assume $C_{ij}(\theta) = \|x_i - g_\theta(z_j)\|_2^2$, but the algorithm can also adopt other metrics. The flowchart of forward and backward propagation is shown in figure 5, and the algorithm is shown in Algorithm 2.

Different from the learning method based on Sinkhorn iterations in [GPC17], the back-propagation in our method does not go into proximal point iterations because the derivative over Γ^* is not needed, which accelerates the learning process greatly. This also has significant implications numerically because the derivative of a computed quantity tends to amplify the error.

Furthermore, we observe the method in [GPC17] suffers shrinkage problem, i.e. the generated distribution tends to shrink towards the target mean. The recovery of target distribution is sensitive to the weight of regularization term ϵ . Only relatively small ϵ can lead to a reasonable generated distribution.

Note Sinkhorn distance is defined as

$$S(\{x_i\}, \{g_\theta(z_j)\}) = \langle \mathbf{C}(\theta), \Gamma^* \rangle,$$

where $\Gamma^* = \arg \min_{\Gamma \in \Sigma(\mathbf{1}/n, \mathbf{1}/n)} \langle \mathbf{C}(\theta), \Gamma \rangle + \epsilon h(\Gamma)$. If Sinkhorn distance is used in learning generative models, envelop theorem cannot be used because the loss function for optimizing θ and Γ is not the

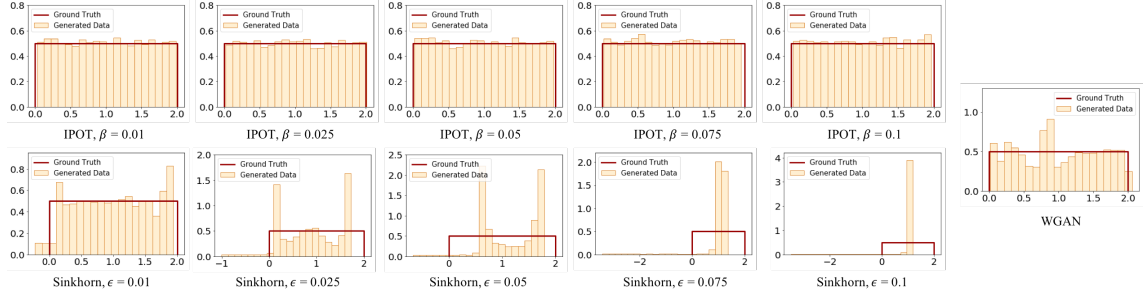


Figure 6: The learning result of IPOT, Sinkhorn, and dual method. In each figure, the orange histogram is the histogram of generated data, while the red line represents the probability distribution function (PDF) of the ground truth.

same. We also try using regularized Wasserstein distance. The regularization term causes much more blur in the following MNIST test, and severer shrinkage problem.

Algorithm 2 Learning generative networks

- 1: **Input:** real data $\{x_i\}$, initialized generator g_θ
 - 2: **while** not converged **do**
 - 3: Sample a batch of real data $\{x_i\}_{i=1}^n$
 - 4: Sample a batch of noise data $\{z_j\}_{i=1}^n \sim q$
 - 5: $C_{ij} := c(x_i, g_\theta(z_j)) := \|x_i - g_\theta(z_j)\|_2^2$
 - 6: $G_{ij} \leftarrow e^{-\frac{C_{ij}}{\epsilon}}$
 - 7: $\Gamma^{(1)} \leftarrow \mathbf{1}\mathbf{1}^T$
 - 8: $\mathbf{v} \leftarrow \frac{1}{n}\mathbf{1}_n$
 - 9: $\mathbf{b} \leftarrow \mathbf{v}$
 - 10: **for** $t = 1, 2, 3, \dots$ **do**
 - 11: $\mathbf{Q} \leftarrow \mathbf{G} \odot \Gamma^{(t)}$
 - 12: **for** $l = 1, 2, 3, \dots, L$ **do** // Usually set $L = 1$
 - 13: $\mathbf{a} \leftarrow \frac{\mathbf{v}}{\mathbf{Q}\mathbf{b}}, \mathbf{b} \leftarrow \frac{\mathbf{v}}{\mathbf{Q}^T\mathbf{a}}$
 - 14: **end for**
 - 15: $\Gamma^{(t+1)} \leftarrow \text{diag}(\mathbf{a})\mathbf{Q}\text{diag}(\mathbf{b})$
 - 16: Update θ with $\langle \Gamma, [2(x_i - g_\theta(z_j)) \frac{\partial g_\theta(z_j)}{\partial \theta}] \rangle$
-

5.1 Experiments on 1D Synthetic Data

First, we do a 1D toy example. The source and target data both follows uniform distribution. The test use 50000 uniformly distributed data. The generators are all 1D-1D NN with one hidden layer. The inner iteration number of IPOT and Sinkhorn are both set to be 200, except in Sinkhorn $\epsilon = 0.01$ case we use 500 because fewer iterations cannot generate reasonable results. While IPOT can typically generate good result in 1 min, Sinkhorn and dual methods usually takes at least tens of minutes. Although when $\epsilon = 0.01$ the code sometimes runs into overflow, we adopt the version without stabilizing because it is quicker. The implementation of dual method (i.e. WGAN method) follows [ACB17].

In figure 6 we show the results. The upper sequence is IPOT with $\beta = 0.01, 0.025, 0.05, 0.075, 0.1$. The results barely change w.r.t. β . The lower sequence is the corresponding Sinkhorn results. Due to smoothing caused by regularization, the result of Sinkhorn method tends to shrink towards the mean, and so the learned distribution cannot cover all the support of target distribution. To demonstrate the reason of this trend, consider the extreme condition when $\epsilon \rightarrow \infty$, the loss function become

$$\Gamma^* = \arg \min_{\Gamma} h(\Gamma) = \arg \min_{\Gamma} D_h(\Gamma, \mathbf{1}\mathbf{1}^T).$$

So $\Gamma^* = \mathbf{1}\mathbf{1}^T$. If we view $\{x_i\}$ and $\{y_j : y_j = g_\theta(z_j)\}$ as the realizations of random variables X and

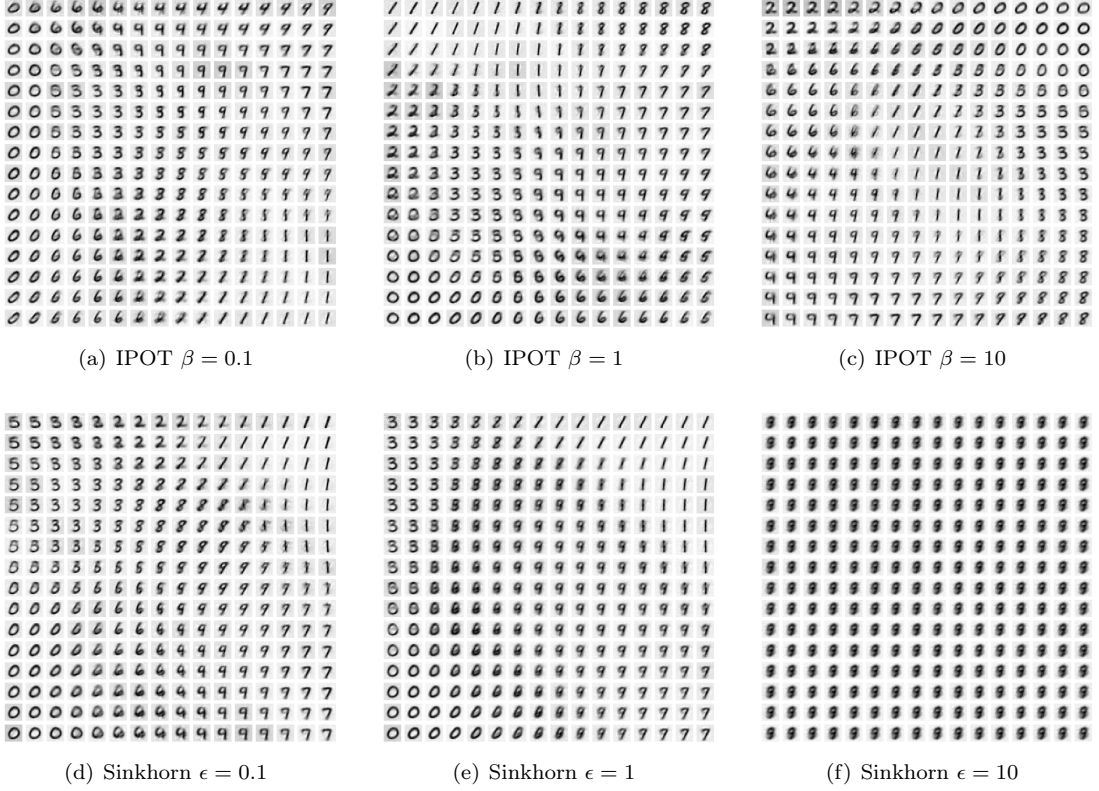


Figure 7: Plots of MNIST learning result under comparable resources. They both use batch size=200, number of hidden layer=1, number of nodes of hidden layer=500, number of iteration=500, learning rate = 1e-4.

Y , the optimal regularized Wasserstein distance W_ϵ from Sinkhorn algorithm is expected to be

$$\begin{aligned} \mathbb{E}_{X,Y}[W_\epsilon] &= \mathbb{E}_{X,Y}[\langle \Gamma^*, \mathbf{C} \rangle] = \mathbb{E}_{X,Y}[\sum_{i,j} (x_i - y_j)^2] \\ &= n^2(\text{Var}(X) + (\bar{X} - \bar{Y})^2 + \text{Var}(Y)), \end{aligned}$$

where n is the data size, $\bar{(\cdot)}$ is the mean of random variable, and $\text{Var}(\cdot)$ is the variance. At the minimum of Wasserstein distance, the mean of generated data $\{y_j\}$ is the same as $\{x_i\}$, but the variance is zero. Therefore, a large ϵ would cause the learned distribution shrink toward the data mean.

5.2 Experiments on Real Data

5.2.1 MNIST Test

Figure 7 shows the generated result for MNIST dataset. The generator $g_\theta : \mathbb{R}^2 \mapsto \mathbb{R}^{784}$ use 2D noise data $\{z_j\} \sim \text{Unif}([0, 1]^2)$ as input, and one fully connected hidden layer with 500 nodes. The images shown in figure 7 is generated by uniform grid points on $[0, 1]^2$, to demonstrate how the latent space is mapped to images.

IPOT generator maps the latent space to all ten digits, while the same shrinkage of Sinkhorn method can be observed in MNIST data as well. While $\epsilon = 0.1$ covers most shapes of the digits, $\epsilon = 1$ only covers a fraction, and $\epsilon = 10$ seems to cover only the mean of images.

This test is for demonstration purpose to argue for the potential of the method, so we do not pursue a performance of state-of-art. For future improvement, a more sophisticated network should be adopted. Also, Euclidean distance as we used here might not be able to capture the structure of high dimension data, especially RGB images. A proper distance would largely improve the capability of the learning model.

6 Extension to Wasserstein Barycenter

Wasserstein barycenter is widely used in machine learning and computer vision due to its nice property [RPDB11, BCC⁺15]. Given a set of distributions $\mathcal{P} = \{\mathbf{p}_1, \mathbf{p}_2, \dots, \mathbf{p}_K\}$, their Wasserstein barycenter is defined as

$$\mathbf{q}^*(\mathcal{P}, \boldsymbol{\lambda}) = \arg \min_{\mathbf{q} \in \mathcal{Q}} \sum_{k=1}^K \lambda_k W(\mathbf{q}, \mathbf{p}_k) \quad (8)$$

where W is the Wasserstein distance, and \mathcal{Q} is in the space of probability distributions, and $\sum_{k=1}^K \lambda_k = 1$.

The idea of our IPOT method can be generalized to learn Wasserstein barycenter. In particular, plugging the definition of Wasserstein distance in (1) into (8) with some derivation (see supplementary material for more), we get the proximal point iteration for barycenter analogous to (5) is

$$\begin{aligned} \{\boldsymbol{\Gamma}_k^{(t+1)}\} &= \arg \min_{\{\boldsymbol{\Gamma}_k\}} \sum_{k=1}^K \lambda_k \{ \langle \boldsymbol{\Gamma}_k, \mathbf{C} \rangle + \beta^{(t)} D_h(\boldsymbol{\Gamma}_k, \boldsymbol{\Gamma}_k^{(t)}) \} \\ \text{s.t. } \boldsymbol{\Gamma}_k \mathbf{1} &= \mathbf{p}_k, \text{ and } \exists \mathbf{q}, \boldsymbol{\Gamma}_k^T \mathbf{1} = \mathbf{q} \end{aligned}$$

The minimization in each proximal step is solved by Sinkhorn barycenter iteration [BCC⁺15], as shown in Algorithm 3. The same as Algorithms 1 and 2, this algorithm can also converge with $L = 1$ and a large range of β . In programming, the steps can be modified to have better efficiency. Please see our code for detail.

Algorithm 3 Computing Wasserstein barycenter

- 1: **Input:** The probability vector set $\{\mathbf{p}_k\}$ on grid $\{y_i\}_{i=1}^n$
 - 2: $\mathbf{b}_k \leftarrow \frac{1}{n} \mathbf{1}_n, \forall k = 1, 2, \dots, K$
 - 3: $C_{ij} \leftarrow c(y_i, y_j) := \|y_i - y_j\|_2^2$
 - 4: $G_{ij} \leftarrow e^{-\frac{C_{ij}}{\beta}}$
 - 5: $\boldsymbol{\Gamma}_k \leftarrow \mathbf{1} \mathbf{1}^T$
 - 6: **for** $t = 1, 2, 3, \dots$ **do**
 - 7: $\mathbf{H}_k \leftarrow \mathbf{G} \odot \boldsymbol{\Gamma}_k, \forall k = 1, 2, \dots, K$
 - 8: **for** $l = 1, 2, 3, \dots, L$ **do**
 - 9: $\mathbf{a}_k \leftarrow \frac{\mathbf{q}}{\mathbf{H}_k \mathbf{b}_k}, \forall k = 1, 2, \dots, K,$
 - 10: $\mathbf{b}_k \leftarrow \frac{\mathbf{p}_k}{\mathbf{H}_k^T \mathbf{a}_k}, \forall k = 1, 2, \dots, K$
 - 11: $\mathbf{q} \leftarrow \prod_{k=1}^K (\mathbf{a}_k \odot (\mathbf{H}_k \mathbf{b}_k))^{\lambda_k}$
 - 12: $\boldsymbol{\Gamma}_k \leftarrow \text{diag}(\mathbf{a}_k) \mathbf{H}_k \text{diag}(\mathbf{b}_k), \forall k = 1, 2, \dots, K$
 - 13: **Return** \mathbf{q}
-

6.1 Learning Barycenter

We test our proximal point barycenter algorithm on MNIST dataset, borrowing the idea from [CD14]. Here, the images in MNIST dataset is randomly uniformly reshape to half to double of its original size, and the reshaped images have random bias towards corner. After that, the images are mapped into 50×50 grid. For each digit we use 50 of the reshaped images as the dataset to compute the barycenter. The weights are set uniform. All results are computed using 50 iterations and under $\epsilon = 0.001$. The results are shown in figure 8. The results from proximal point algorithm are clear, while the results of Sinkhorn based algorithms suffer blurry effect due to entropic regularization.

While the time complexity of our method is in the same order of magnitude with Sinkhorn algorithm [BCC⁺15], the space complexity is K times of it, because K different transport maps need to be stored. If K is large, this might cause pressure to RAM. Therefore, a sequential method is needed. We left this to future work.

7 Color Transferring

Optimal transport is directly applicable to many applications, such as color transferring and histogram calibration. We will show the result of color transferring and why accurate transportation

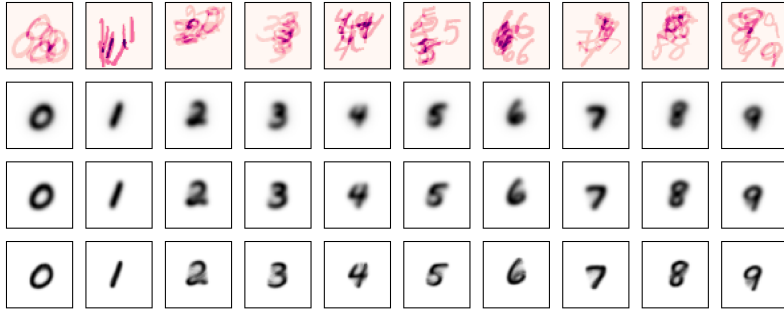


Figure 8: The result of barycenter. For each digit, we randomly choose 8 of 50 scaled and shifted images to demonstrate the input data. From the top to the bottom, we show (top row) the demo of input data; (second row) the results based on [CD14]; (third row) the result based on [BCC+15]; (bottom row) the results based on inexact proximal point algorithm.

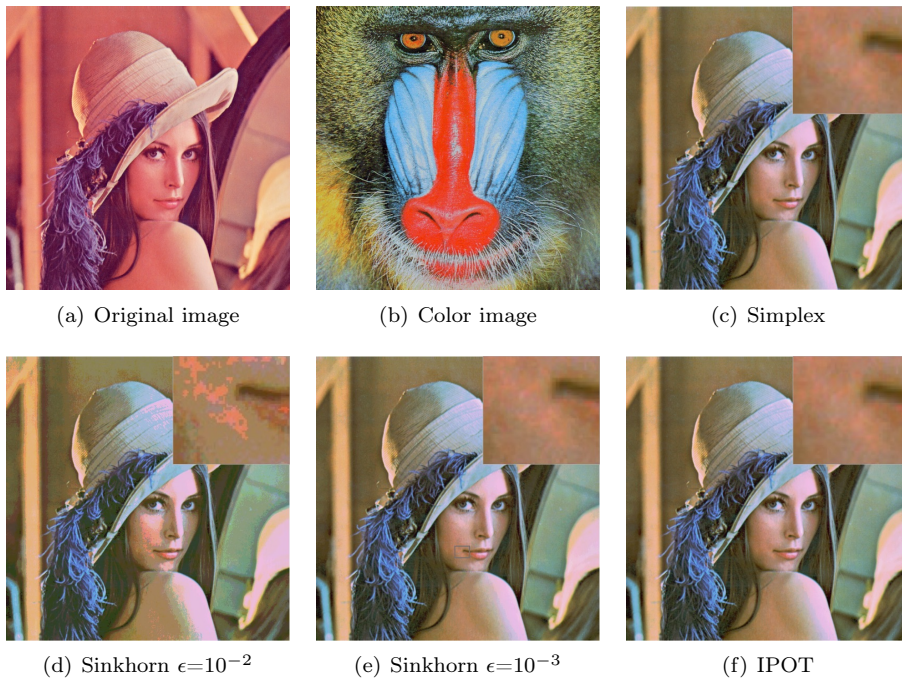


Figure 9: An example of color transferring. The right upper corner of each generated image shows the zoom-in of the color detail of the mouth corner.

map is superior to entropically regularized ones.

The goal of color transferring is to transfer the tonality of a target image into a source image. This is usually done by imposing the histogram of the color palette of one image to another image. Since Reinhard et al. [RAGS01], many methods [RFP14, XM06] are developed to do so by learning the transformation between the two histograms. Experiments in [RTG98] have shown that transformation based on optimal transport map outperforms state-of-the-art techniques for challenging images. Same as other prime-form Wasserstein distance solvers [PW09, Cut13], the proximal method provide a transportation map. By definition, the map is a transportation from the source distribution to a target one with minimum cost. Therefore it provides a way to transform a histogram to another.

One example is shown in figure 9. We use three different maps to transform the RGB channels, respectively. For each channel, there are at most 256 bins. Therefore, using three channels separately is more efficient than treating the colors as 3D data. Figure 9 shows proximal method can produce identical result as linear programming at convergence, while the results produced by Sinkhorn method differ w.r.t. ϵ .

8 Conclusion

We proposed a proximal point method - IPOT - based on Bregman distance to solve optimal transport problem. The algorithm can converge to ground truth even if the inner optimization iteration only performs a few times. We also demonstrate its potential in generative models and Wasserstein barycenter. For generative models, we show the back-propagation of learning process based on proximal point method can be largely simplified by envelop theorem. For barycenter, our new method can generate much sharper results than state-of-art.

References

- [ACB17] Martin Arjovsky, Soumith Chintala, and Léon Bottou. Wasserstein generative adversarial networks. In *International Conference on Machine Learning*, pages 214–223, 2017.
- [Afr71] SN Afriat. Theory of maxima and the method of Lagrange. *SIAM Journal on Applied Mathematics*, 20(3):343–357, 1971.
- [AWR17] Jason Altschuler, Jonathan Weed, and Philippe Rigollet. Near-linear time approximation algorithms for optimal transport via Sinkhorn iteration. *arXiv preprint arXiv:1705.09634*, 2017.
- [BCC⁺15] Jean-David Benamou, Guillaume Carlier, Marco Cuturi, Luca Nenna, and Gabriel Peyré. Iterative Bregman projections for regularized transportation problems. *SIAM Journal on Scientific Computing*, 37(2):A1111–A1138, 2015.
- [BJGR17] Espen Bernton, Pierre E Jacob, Mathieu Gerber, and Christian P Robert. Inference in generative models using the Wasserstein distance. *arXiv preprint arXiv:1701.05146*, 2017.
- [CD14] Marco Cuturi and Arnaud Doucet. Fast computation of Wasserstein barycenters. In *International Conference on Machine Learning*, pages 685–693, 2014.
- [CPSV16] Lenaïc Chizat, Gabriel Peyré, Bernhard Schmitzer, and François-Xavier Vialard. Scaling algorithms for unbalanced transport problems. *arXiv preprint arXiv:1607.05816*, 2016.
- [Cut13] Marco Cuturi. Sinkhorn distances: Lightspeed computation of optimal transport. In *Advances in neural information processing systems*, pages 2292–2300, 2013.
- [DOT17] Pavel Dvurechensky, Sergey Omelchenko, and Alexander Tiurin. Adaptive similar triangles method: a stable alternative to Sinkhorn’s algorithm for regularized optimal transport. *arXiv preprint arXiv:1706.07622*, 2017.
- [Eck93] Jonathan Eckstein. Nonlinear proximal point algorithms using bregman functions, with applications to convex programming. *Mathematics of Operations Research*, 18(1):202–226, 1993.
- [Eck98] Jonathan Eckstein. Approximate iterations in bregman-function-based proximal algorithms. *Mathematical programming*, 83(1-3):113–123, 1998.
- [FC17] Rémi Flamary and Nicolas Courty. Pot python optimal transport library. 2017.
- [FL89] Joel Franklin and Jens Lorenz. On the scaling of multidimensional matrices. *Linear Algebra and its applications*, 114:717–735, 1989.
- [GPAM⁺14] Ian Goodfellow, Jean Pouget-Abadie, Mehdi Mirza, Bing Xu, David Warde-Farley, Sherjil Ozair, Aaron Courville, and Yoshua Bengio. Generative adversarial nets. In *Advances in neural information processing systems*, pages 2672–2680, 2014.
- [GPC17] Aude Genevay, Gabriel Peyré, and Marco Cuturi. Sinkhorn-AutoDiff: Tractable Wasserstein learning of generative models. *arXiv preprint arXiv:1706.00292*, 2017.

- [Kan42] LV Kantorovich. On mass transfer problem. *Dokl. Acad. Nauk SSSR*37, pages 199–201, 1942.
- [MHAH⁺16] Manuel Martinez, Monica Haurilet, Ziad Al-Halah, Makarand Tapaswi, and Rainer Stiefelhagen. Relaxed earth mover’s distances for chain-and tree-connected spaces and their use as a loss function in deep learning. *arXiv preprint arXiv:1611.07573*, 2016.
- [PB⁺14] Neal Parikh, Stephen Boyd, et al. Proximal algorithms. *Foundations and Trends® in Optimization*, 1(3):127–239, 2014.
- [Pol87] B. Polyak. *Introduction to optimization*. Optimization Software Inc., New York, 1987.
- [PW09] Ofir Pele and Michael Werman. Fast and robust earth mover’s distances. In *Computer vision, 2009 IEEE 12th international conference on*, pages 460–467. IEEE, 2009.
- [RAGS01] Erik Reinhard, Michael Adhikhmin, Bruce Gooch, and Peter Shirley. Color transfer between images. *IEEE Computer graphics and applications*, 21(5):34–41, 2001.
- [RFP14] Julien Rabin, Sira Ferradans, and Nicolas Papadakis. Adaptive color transfer with relaxed optimal transport. In *Image Processing (ICIP), 2014 IEEE International Conference on*, pages 4852–4856. IEEE, 2014.
- [Roc76a] R Tyrrell Rockafellar. Augmented Lagrangians and applications of the proximal point algorithm in convex programming. *Mathematics of operations research*, 1(2):97–116, 1976.
- [Roc76b] R Tyrrell Rockafellar. Monotone operators and the proximal point algorithm. *SIAM journal on control and optimization*, 14(5):877–898, 1976.
- [RPDB11] Julien Rabin, Gabriel Peyré, Julie Delon, and Marc Bernot. Wasserstein barycenter and its application to texture mixing. In *International Conference on Scale Space and Variational Methods in Computer Vision*, pages 435–446. Springer, 2011.
- [RTG98] Yossi Rubner, Carlo Tomasi, and Leonidas J Guibas. A metric for distributions with applications to image databases. In *Computer Vision, 1998. Sixth International Conference on*, pages 59–66. IEEE, 1998.
- [Sch16] Bernhard Schmitzer. Stabilized sparse scaling algorithms for entropy regularized transport problems. *arXiv preprint arXiv:1610.06519*, 2016.
- [SRB11] Mark Schmidt, Nicolas L Roux, and Francis R Bach. Convergence rates of inexact proximal-gradient methods for convex optimization. In *Advances in neural information processing systems*, pages 1458–1466, 2011.
- [SS01] MV Solodov and Benar Fux Svaiter. A unified framework for some inexact proximal point algorithms. 2001.
- [SZ17] A. M.-C. So and Z. Zhou. Non-asymptotic convergence analysis of inexact gradient methods for machine learning without strong convexity. *Optimization Methods and Software*, 32(4):963–992, 2017.
- [TCDP17] Alexis Thibault, Lénaïc Chizat, Charles Dossal, and Nicolas Papadakis. Overrelaxed Sinkhorn-Knopp algorithm for regularized optimal transport. *arXiv preprint arXiv:1711.01851*, 2017.
- [Teb92] Marc Teboulle. Entropic proximal mappings with applications to nonlinear programming. *Mathematics of Operations Research*, 17(3):670–690, 1992.
- [TPK⁺17] Matthew Thorpe, Serim Park, Soheil Kolouri, Gustavo K Rohde, and Dejan Slepčev. A transportation L^p distance for signal analysis. *Journal of Mathematical Imaging and Vision*, 59(2):187–210, 2017.
- [XM06] Xuezhong Xiao and Lizhuang Ma. Color transfer in correlated color space. In *Proceedings of the 2006 ACM international conference on Virtual reality continuum and its applications*, pages 305–309. ACM, 2006.

A General Bregman Proximal Point Algorithm

In the main body of the paper, we discussed the proximal point algorithm with specific Bregman distance, which is generated through the traditional entropy function. In this section, we generalize our results by proving the effectiveness of proximal point algorithm with general Bregman distance. Bregman distance is applied to measure the discrepancy between different matrices which turns out to be one of the key ideas in regularized optimal transport problems. Its special structure also give rise to proximal-type algorithms and projectors in solving optimization problems.

A.1 Basic Algorithm Framework and Preliminaries

The fundamental iterative scheme of general Bregman proximal point algorithm can be denoted as

$$x^{(t+1)} = \arg \min_{x \in X} \left\{ f(x) + \beta^{(t)} D_h(x, x^{(t)}) \right\}, \quad (9)$$

where $t \in \mathbb{N}$ is the index of iteration, and $D_h(x, x^{(t)})$ denotes a general Bregman distance between x and $x^{(t)}$ based on a Legendre function h (The definition is presented in the following). In the main body of the paper, h is specialized as the classical entropy function and as follows the related Bregman distance reduces to the generalized KL divergence. Furthermore, the Sinkhorn-Knopp projection can be introduced to calculate each iterative subproblem. In the following, we present some fundamental definitions and lemmas.

Definition A.1. *Legendre function:* Let $h : X \rightarrow (-\infty, \infty]$ be a lsc proper convex function. It is called

1. Essentially smooth: if h is differentiable on $\text{int dom } h$, with moreover $\|\nabla h(x^{(t)})\| \rightarrow \infty$ for every sequence $\{x^{(t)}\} \subset \text{int dom } h$ converging to a boundary point of $\text{dom } h$ as $t \rightarrow +\infty$;
2. Legendre type: if h is essentially smooth and strictly convex on $\text{int dom } h$.

Definition A.2. *Bregman distance:* any given Legendre function h ,

$$D_h(x, y) = h(x) - h(y) - \langle \nabla h(y), x - y \rangle, \quad \forall x \in \text{dom } h, \forall y \in \text{int dom } h, \quad (10)$$

where D_h is strictly convex with respect to its first argument. Moreover, $D_h(x, y) \geq 0$ for all $(x, y) \in \text{dom } h \times \text{int dom } h$, and it is equal to zero if and only if $x = y$. However, D_h is in general asymmetric, i.e., $D_h(x, y) \neq D_h(y, x)$.

Definition A.3. *Symmetry Coefficient:* Given a Legendre function $h : X \rightarrow (-\infty, \infty]$, its symmetry coefficient is defined by

$$\alpha(h) = \inf \left\{ \frac{D_h(x, y)}{D_h(y, x)} \mid (x, y) \in \text{int dom } h \times \text{int dom } h, x \neq y \right\} \in [0, 1]. \quad (11)$$

Lemma A.4. *Given $h : X \rightarrow (-\infty, +\infty]$, D_h is general Bregman distance, and $x, y, z \in X$ such that $h(x), h(y), h(z)$ are finite and h is differentiable at y and z ,*

$$D_h(x, z) - D_h(x, y) - D_h(y, z) = \langle \nabla h(y) - \nabla h(z), x - y \rangle \quad (12)$$

Proof. The proof is straightforward as one can easily verify it by simply subtracting $D_h(y, z)$ and $D_h(x, y)$ from $D_h(x, z)$. \square

A.2 Theorem 3.1 and Theorem 3.2

In this section, we first establish the convergence of Bregman proximal point algorithm, i.e., **Theorem 3.1**, while our analysis is based on ([Eck93, Teb92, Eck98]). Further, we establish the convergence of inexact version Bregman proximal point algorithm, i.e., **Theorem 3.2**, in which the subproblem in each iteration is computed inexactly within finite number of sub-iterations. Before proving both theorems, we propose several fundamental lemmas. The first Lemma is the fundamental descent lemma, which is popularly used to analysis the convergence result of first-order methods.

Lemma A.5. (*Descent Lemma*) Consider a closed proper convex function $f : X \rightarrow (-\infty, \infty]$ and for any $x \in X$ and $\beta^{(t)} > 0$, we have:

$$f(x^{(t+1)}) \leq f(x) + \beta^{(t)} \left[D_h(x, x^{(t)}) - D_h(x, x^{(t+1)}) - D_h(x^{(t+1)}, x^{(t)}) \right], \quad \forall x \in X. \quad (13)$$

Proof. The optimality condition of (9) can be written as

$$(x - x^{(t+1)})^T \left[\nabla f(x^{(t+1)}) + \beta^{(t)} (\nabla h(x^{(t+1)}) - \nabla h(x^{(t)})) \right] \geq 0, \quad \forall x \in X.$$

Then with the convexity of f , we obtain

$$f(x) - f(x^{(t+1)}) + \beta^{(t)} (x - x^{(t+1)})^T (\nabla h(x^{(t+1)}) - \nabla h(x^{(t)})) \geq 0. \quad (14)$$

With (12) it follows that

$$(x - x^{(t+1)})^T (\nabla h(x^{(t+1)}) - \nabla h(x^{(t)})) = D_h(x, x^{(t)}) - D_h(x, x^{(t+1)}) - D_h(x^{(t+1)}, x^{(t)}).$$

Substitute the above equation into (14), we have

$$f(x^{(t+1)}) \leq f(x) + \beta^{(t)} \left[D_h(x, x^{(t)}) - D_h(x, x^{(t+1)}) - D_h(x^{(t+1)}, x^{(t)}) \right], \quad \forall x \in X.$$

□

Next, we prove the convergence result in **Theorem 3.1**.

Theorem 3.1 Let $\{x^{(t)}\}$ be the sequence generated by the general Bregman proximal point algorithm with iteration (9) where f is assumed to be continuous and convex. Further assume that $f^* = \min f(x) > -\infty$. Then we have that $\{f(x^{(t)})\}$ is non-increasing, and $f(x^{(t)}) \rightarrow f^*$. Further assume there exists η , s.t.

$$f^* + \eta d(x) \leq f(x), \quad \forall x \in X, \quad (15)$$

The algorithm has linear convergence.

Proof. 1. First, we prove the sufficient decrease property:

$$f(x^{(t+1)}) \leq f(x^{(t)}) - \beta^{(t)} (1 + \alpha(h)) D_h(x^{(t+1)}, x^{(t)}). \quad (16)$$

Let $x = x^{(t)}$ in (13), we obtain

$$\begin{aligned} f(x^{(t+1)}) &\leq f(x^{(t)}) - \beta^{(t)} \left[D_h(x^{(t)}, x^{(t+1)}) + D_h(x^{(t+1)}, x^{(t)}) \right] \\ &\leq f(x^{(t)}) - \beta^{(t)} (1 + \alpha(h)) D_h(x^{(t+1)}, x^{(t)}). \end{aligned}$$

With the sufficient decrease property, it is obvious that $\{f(x^{(t)})\}$ is non-increasing.

2. Summing (16) from $i = 0$ to $i = t - 1$ and for simplicity assuming $\beta^{(t)} = \beta$, we have

$$\begin{aligned} \sum_{i=0}^{t-1} \left[\frac{1}{\beta^{(t)}} \left(f(x^{(i+1)}) - f(x^{(i)}) \right) \right] &\leq - [1 + \alpha(h)] \sum_{i=0}^{t-1} D_h(x^{(i+1)}, x^{(i)}) \\ \Rightarrow \sum_{i=0}^{\infty} D_h(x^{(i+1)}, x^{(i)}) &< \frac{1}{\beta(1 + \alpha(h))} f(x^{(0)}) < \infty, \end{aligned}$$

which indicates that $D_h(x^{(i+1)}, x^{(i)}) \rightarrow 0$. Then summing (13) from $i = 0$ to $i = t - 1$, we have

$$k \left(f(x^{(t)}) - f(x) \right) \leq \sum_{i=0}^{t-1} \left(f(x^{(i+1)}) - f(x) \right) \leq \beta D_h(x, x^{(0)}) < \infty, \quad \forall x \in X.$$

Let $t \rightarrow \infty$, we have $\lim_{t \rightarrow \infty} f(x^{(t)}) \leq f(x)$ for every x , as a result we have $\lim_{k \rightarrow \infty} f(x^{(k)}) = f^*$.

3. Finally, we prove the convergence rate is linear. Assume $x^* = \arg \min_x f(x)$ is the unique optimal solution. Denote $d(x) = D_h(x^*, x)$. Let also $\beta^{(t)} = \beta$, we will prove

$$\frac{d(x^{(t+1)})}{d(x^{(t)})} \leq \frac{1}{1 + \frac{\eta}{\beta}} \quad (17)$$

Replace x with x^* in inequality (13), we have

$$f(x^{(t+1)}) \leq f^* + \beta \left[d(x^{(t)}) - d(x^{(t+1)}) - D_h(x^{(t+1)}, x^{(t)}) \right]. \quad (18)$$

Using assumption 15, we have

$$f^* + \eta d(x^{(t+1)}) \leq f(x^{(t+1)}) \quad (19)$$

Sum 18 and 19 up, we have

$$\begin{aligned} \frac{\eta}{\beta} d(x^{(t+1)}) &\leq d(x^{(t)}) - d(x^{(t+1)}) - D_h(x^{(t+1)}, x^{(t)}) \\ &\leq d(x^{(t)}) - d(x^{(t+1)}) \end{aligned}$$

Therefore,

$$\frac{d(x^{(t+1)})}{d(x^{(t)})} \leq \frac{1}{1 + \frac{\eta}{\beta}}$$

Therefore, we have a linear convergence in Bregman distance sense. \square

Unfortunately, assumption (15) does not always hold when f is linear. However, in our specific case, Γ is bounded in $[0, 1]^{n \times n}$. In this case, for η to exist, we only need

$$\lim_{\Gamma \rightarrow \Gamma^*} \frac{D_h(\Gamma^*, \Gamma)}{\langle C, \Gamma^* - \Gamma \rangle} < \infty$$

Easy to prove the above holds.

Inequality (17) shows how the convergence rate is linked to β . This is the reason we claim in Section 4.1 that a smaller β would lead to quicker convergence in exact case.

From above, we showed that the general Bregman proximal point algorithm with constant stepsize can guarantee convergence to the optimal solution f^* , and has linear convergence rate with some assumptions. Further, we prove the convergence result for the general Bregman proximal point algorithm with inexact scheme in **Theorem 3.2**.

Theorem 3.2 *Let $\{x^{(t)}\}$ be the sequence generated by the general Bregman proximal point algorithm with inexact scheme (i.e., finite number of inner iterations are employed). Define an error sequence $\{e^{(t)}\}$ where*

$$e^{(t+1)} \in \beta^{(t)} \left[\nabla f(x^{(t+1)}) + \partial \iota_X(x^{(t+1)}) \right] + \left[\nabla h(x^{(t+1)}) - \nabla h(x^{(t)}) \right], \quad (20)$$

where ι_X is the indicator function of set X . If the sequence $\{e^{(t)}\}$ satisfies $\sum_{k=1}^{\infty} \|e^{(k)}\| < \infty$ and $\sum_{k=1}^{\infty} \langle e^{(k)}, x^{(k)} \rangle$ exists and is finite, then $\{x^{(t)}\}$ converges to x^∞ with $f(x^\infty) = f^*$. If the sequence $\{e^{(t)}\}$ satisfies that exist $\rho \in (0, 1)$ such that $\|e^{(t)}\| \leq \rho^t$, $\langle e^{(t)}, x^{(t)} \rangle \leq \rho^t$ and with assumption (15), then $\{x^{(t)}\}$ converges linearly.

Remark: If exact minimization is guaranteed in each iteration, the sequence $\{x^{(t)}\}$ will satisfy that

$$0 \in \beta^{(t)} \left[\nabla f(x^{(t+1)}) + \partial \iota_X(x^{(t+1)}) \right] + \frac{1}{\beta^{(t)}} \left[\nabla h(x^{(t+1)}) - \nabla h(x^{(t)}) \right].$$

As a result, with enough inner iteration, the guaranteed $e^{(t)}$ will goes to zero.

Proof. This theorem is extended from [Eck98, Theorem 1], and we propose a brief proof here. The proof contains the following four steps:

1. We have for all $k \geq 0$, through the three point lemma

$$D_h(x, x^{(t+1)}) = D_h(x, x^{(t)}) - D_h(x^{(t+1)}, x^{(t)}) - \langle \nabla h(x^{(t)}) - \nabla h(x^{(t+1)}), x^{(t+1)} - x \rangle,$$

which indicates

$$D_h(x, x^{(t+1)}) = D_h(x, x^{(t)}) - D_h(x^{(t+1)}, x^{(t)}) - \langle \nabla h(x^{(t)}) - \nabla h(x^{(t+1)}) + e^{(t+1)}, x^{(t+1)} - x \rangle + \langle e^{(t+1)}, x^{(t+1)} - x \rangle.$$

Since $\frac{1}{\beta^{(t)}} [e^{(t+1)} + \nabla h(x^{(t)}) - \nabla h(x^{(t+1)})] \in \nabla f(x^{(t+1)}) + \partial \iota_X(x^{(t+1)})$ and $0 \in \nabla f(x^*) + \partial \iota_X(x^*)$ if x^* be the optimal solution, we have

$$\begin{aligned} & \langle \nabla h(x^{(t)}) - \nabla h(x^{(t+1)}) + e^{(t+1)}, x^{(t+1)} - x^* \rangle \\ &= \beta^{(t)} \left\langle \left[\frac{1}{\beta^{(t)}} \left(\nabla h(x^{(t)}) - \nabla h(x^{(t+1)}) + e^{(t+1)} \right) \right] - 0, x^{(t+1)} - x^* \right\rangle \geq 0, \end{aligned}$$

because $\nabla f + \partial \iota_X$ is monotone ($f + \iota_X$ is convex). Further we have

$$D_h(x^*, x^{(t+1)}) \leq D_h(x^*, x^{(t)}) - D_h(x^{(t+1)}, x^{(t)}) + \langle e^{(t+1)}, x^{(t+1)} - x^* \rangle.$$

2. Summing the above inequality from $i = 0$ to $i = t - 1$, we have

$$D_h(x^*, x^{(t)}) \leq D_h(x^*, x^{(0)}) - \sum_{i=0}^{t-1} D_h(x^{(i+1)}, x^{(i)}) + \sum_{i=0}^{t-1} \langle e^{(i+1)}, x^{(i+1)} - x^* \rangle.$$

Since $\sum_{t=1}^{\infty} \|e^{(t)}\| < \infty$ and $\sum_{t=1}^{\infty} \langle e^{(t)}, x^{(t)} \rangle$ exists and is finite, we guarantee that

$$\bar{E}(x^*) = \sup_{t \geq 0} \left\{ \sum_{i=0}^{t-1} \langle e^{(i+1)}, x^{(i+1)} - x^* \rangle \right\} < \infty.$$

Together with $D_h(x^{(i+1)}, x^{(i)}) > 0$, we have

$$D_h(x^*, x^{(t)}) \leq D_h(x^*, x^{(0)}) + \bar{E}(x^*) < \infty,$$

which indicates

$$0 \leq \sum_{i=0}^{\infty} D_h(x^{(i+1)}, x^{(i)}) < D_h(x^*, x^{(0)}) + \bar{E}(x^*) < \infty,$$

and hence $D_h(x^{(i+1)}, x^{(i)}) \rightarrow 0$.

3. Based on the above two items, we know that the sequence $\{x^{(t)}\}$ must be bounded and has at least one limit point x^∞ . The most delicate part of the proof is to establish that $0 \in \nabla f(x^\infty) + \partial \iota_X(x^\infty)$. Let $T = \nabla f + \partial \iota_X$, then T denotes the subdifferential mapping of a closed proper convex function $f + \iota_X$ (f is a linear function and X is a closed convex set). Let $\{t_j\}$ be the subsequence such that $x^{t_j} \rightarrow x^\infty$. Because $x^{t_j} \in X$ and X is a closed convex set, we know $x^\infty \in X$. We know that $D_h(x^*, x^{(t+1)}) \leq D_h(x^*, x^{(t)}) + \langle e^{(t+1)}, x^{(t+1)} - x^* \rangle$ and $\sum_{k=0}^{\infty} \langle e^{(k+1)}, x^{(k+1)} - x^* \rangle$ exists and is finite. From [Pol87, Section 2.2], we guarantee that $\{D_h(x^*, x^{(t)})\}$ converges to $0 \leq d(x^*) < \infty$. Define $y^{(t+1)} := \lambda_k \left(\nabla h(x^{(t)}) - \nabla h(x^{(t+1)}) + e^{(t+1)} \right)$, we have

$$\lambda_k \langle y^{(t+1)}, x^{(t+1)} - x^* \rangle = D_h(x^*, x^{(t)}) - D_h(x^*, x^{(t+1)}) - D_h(x^{(t+1)}, x^{(t)}) + \langle e^{(t+1)}, x^{(t+1)} - x^* \rangle.$$

By taking the limit of both sides and $\lambda_k = \lambda > 0$, we obtain that

$$\langle y^{(t+1)}, x^{(t+1)} - x^* \rangle \rightarrow 0.$$

For the reason that y^{k_j+1} is a subgradient of $f + \iota_X$ at x^{k_j+1} , we have

$$f(x^*) \geq f(x^{k_j+1}) + \langle y^{k_j+1}, x^* - x^{k_j+1} \rangle, \quad x^* \in X, x^{k_j+1} \in X.$$

Further let $j \rightarrow \infty$ and using f is lower semicontinuous, $\langle y^{(t+1)}, x^{(t+1)} - x^* \rangle \rightarrow 0$, we obtain

$$f(x^*) \geq f(x^\infty), \quad x^\infty \in X$$

which implies that $0 \in \nabla f(x^\infty) + \iota_X(x^\infty)$.

4. Recall the inexact scheme (20), we can equivalently guarantee that

$$(x - x^{(t+1)})^T \left\{ \beta^{(t)} \nabla f(x^{(t+1)}) + \left[\nabla h(x^{(t+1)}) - \nabla h(x^{(t)}) \right] - e^{(t+1)} \right\} \geq 0, \forall x \in X.$$

Together the convexity of f and the three point lemma, we obtain

$$f(x^{(t+1)}) \leq f(x) + \frac{1}{\beta^{(t)}} \left[D_h(x, x^{(t)}) - D_h(x, x^{(t+1)}) - D_h(x^{(t+1)}, x^{(t)}) - (x - x^{(t+1)})^T e^{(t+1)} \right].$$

Let $x = x^*$ in the above inequality and recall the assumption (15), *i.e.*,

$$f(x) - f(x^*) \geq \eta d(x),$$

we have with $\beta^{(t)} = \beta$

$$\begin{aligned} \eta d(x^{(t+1)}) &\leq \frac{1}{\beta} \left[d(x^{(t)}) - d(x^{(t+1)}) \right] + \frac{1}{\beta} \left((x^{(t+1)} - x^*)^T e^{(t+1)} \right) \\ &\leq \frac{1}{\beta} \left[d(x^{(t)}) - d(x^{(t+1)}) \right] + \frac{1}{\beta} \left(C \|e^{(t+1)}\| + \langle x^{(t+1)}, e^{(t+1)} \rangle \right), \end{aligned}$$

where $C := \sup_{x \in X^*} \{\|x\|\}$. The second inequality is obtained through triangle inequality. Then

$$d^{(t+1)} \leq \mu d^{(t)} + \mu \left(C \|e^{(t+1)}\| + \langle x^{(t+1)}, e^{(t+1)} \rangle \right),$$

where $\mu = \frac{1}{1+\beta\eta} < 1$. With our assumptions and according to Theorem 2 and Corollary 2 in [SZ17], we guarantee the generated sequence converges linearly in the order of $\mathcal{O}(c^t)$, where $c = \sqrt{\frac{1+\max\{\mu, \rho\}}{2}} \in (0, 1)$.

Based on the above four items, we guarantee the convergence results in this theorem. \square